International Journal of Nanomedicine

Dovepress

open access to scientific and medical research

Open Access Full Text Article

ORIGINAL RESEARCH

Polydopamine Nanoparticles-Based Photothermal Effect Against Adhesion Formation in a Rat Model of Achilles Tendon Laceration Repair

Zekun Zhou[1,2], Shaoyan Li[1,2], Xu Gong[1,2]

[1]Department of Hand and Podiatric Surgery, Orthopedics Center, The First Hospital of Jilin University, Changchun, 130021, People's Republic of China; [2]Jilin Province Key Laboratory on Tissue Repair, Reconstruction and Regeneration, The First Hospital of Jilin University, Changchun, 130021, People's Republic of China

Correspondence: Xu Gong, Department of Hand and Podiatric Surgery, Orthopedics Center, The First Hospital of Jilin University, Changchun, 130021, People's Republic of China, Tel +86 13944099151, Email gongxu@jlu.edu.cn

Background: Adhesion formation after tendon surgery is a major obstacle to repair of tendon ruptures, and there is still no effective clinical anti-adhesion method. Myofibroblasts expressing α-smooth muscle actin (α-SMA) play a crucial role in adhered fibrous tissue. Heat shock protein (Hsp) 72 can selectively prevent the activation of c-Jun N-terminal kinase (JNK), which mediates the conversion from fibroblasts to myofibroblasts. The purpose of this study was to investigate for the first time whether polydopamine nanoparticles (PDA NPs)-based photothermal effect would attenuate adhesion formation in a rat model of Achilles tendon laceration repair.

Materials and Methods: Forty-five adult male Sprague-Dawley rats were randomly assigned to the photothermal group, the control group and the PDA NPs group (n = 15 per group). The primary outcome measure was the adhesion scores at two weeks after surgery according to the grading of Tang et al. The secondary outcomes included the expressions of Hsp 72, JNK, phosphorylated JNK and α-SMA, which were measured by immunohistochemistry or Western blot.

Results: The average adhesion score was significantly lower in the photothermal group (4.25 ± 0.21) than that in the control group (5.29 ± 0.12) (p = 0.005) and the PDA NPs group (5.29 ± 0.20) (p = 0.005). Relative to the control group and PDA NPs group, Hsp 72 in the photothermal group was significantly increased whereas α-SMA and p-JNK was significantly decreased, but JNK was not found to be different across the three groups.

Conclusion: The photothermal effect produced by PDA NPs could reduce tendon adhesion formation in rats by inhibiting myocyte fibrosis, which may have potential in developing endogenous heating for postsurgical tissue adhesions.

Keywords: adhesion formation, tendon, polydopamine nanoparticle, photothermal effects

Introduction

Tendon is a dense connective tissue with a mechanical function: translating muscular contractions into articular movement by transmitting forces from muscle to bone.[1] Tendon injury is one of the most common injuries in daily living, but its therapeutic outcomes are not satisfactory.[2] A predominant factor affecting outcomes after tendon surgery is adhesion formation, which limits joint motion by disrupting the gliding function of the tendons and frequently results in secondary joint contracture and stiffness. In clinical settings, a major approach to prevent adhesion formation after tendon surgery is early passive or active mobilization, but adhesion formation still occurs in 30% of patients.[2,3] Although a number of preventive strategies including physical barriers, pharmacologic agents and gene therapies etc. have been proposed to attenuate adhesion formation after tendon repair, their beneficial effects have not yet been established in clinical settings.[4–15] Up to now, adhesion formation after tendon injury remains a great challenge for the hand surgeons.

Adhesion formation after tendon injury is a fibrosis between the injured tendons and the surrounding tissues.[16] Injury initiates inflammatory response and inflammatory cells infiltrate into the subcutaneous tissue and the tendon. These inflammatory cells release pro-fibrotic cytokines such as transforming growth factor beta 1 (TGF-β1) and platelet-derived

Received: 15 October 2022
Accepted: 21 March 2023
Published: 4 April 2023

growth factor, etc.[16–18] Among these, TGF-β1 activates and differentiates resident fibroblasts into metabolically active myofibroblasts with α-smooth muscle actin (α-SMA).[16–18] Relative to fibroblasts, myofibroblasts produce more collagenous extracellular matrix and are considered to be a key effector in various fibrotic responses,[19] inhibition of myofibroblasts might be a potential approach for attenuating adhesion formation after tendon injury.

Reich et al have demonstrated that the activation of fibroblasts by TGF-β1 was mediated by intracellular c-Jun N-terminal Kinase (JNK), and selective inhibition of JNK by CC-930 could attenuate skin fibrosis in systemic sclerosis.[17] Likewise, Wang et al have demonstrated that inhibition of JNK/STAT-3 signaling by aspirin could inhibit scarring after tendon injury.[20] Therefore, JNK might be a potential molecular target for inhibiting the proliferation of fibroblasts after tendon injury. It is well known that heat shock protein (Hsp) 72 can prevent the activation of intracellular JNK.[21] Intracellular Hsp 72 can be induced by mild heat shock (41 °C). Thus, mild heat shock might be a potential approach for preventing adhesion formation after tendon injury. Mulhall et al demonstrated that thermal preconditioning before tendon injury could reduce adhesion formation after tendon injury by reducing inflammation via Hsp 72.[22] However, the roles of Hsp 72 induced by postoperative mild heat shock and its potential therapeutic effects have not yet been evaluated.

In the present study, the photothermal properties of PDA NPs was used to reduce tendon in a rat model of the Achilles tendon laceration repair. In vivo experiments results showed that PDA NPs converted the absorbed light into heat when the repair sites were irradiated with near-infrared (NIR) laser postoperatively. We hypothesized that mild heat shock (41°C) would induce the expression of Hsp 72 around the repaired tendons, which in turn inhibit the proliferation of fibroblasts by preventing phosphorylation of JNK. Our primary outcome measure was the adhesion scores at two weeks after surgery according to the grading of Tang et al.[23] The secondary outcomes included changes in the expressions of Hsp 72, JNK, phosphorylated JNK and α-SMA (marker for myofibroblasts).

Materials and Methods

Synthesis of Polydopamine Nanoparticles

To synthesize polydopamine nanoparticles (PDA NPs) with photothermal properties, 0.6 g of dopamine hydrochloride (99.9%; Sigma, Cat# H8502-25G, St. Louis, America) was added to a mixed solution composed of 85 mL of Tris buffer (10 mM, pH 8.50; Macklin, Cat# T819511-25G, Shanghai, China) and 15 mL of absolute ethyl alcohol (99.7%; Sinopharm Chemical Reagent co., Ltd., Cat# 10009297, Beijing, China). After stirred for 24 h at room temperature, the mixture was centrifuged at 8800 r/min for 10 min. Then the precipitate was collected and washed 3 times with deionized water. After drying, 10 mg of PDA solid powder were weighed and phosphate-buffered saline (PBS) (0.01M, pH 7.2–7.4; Hyclone, Cat# SH30256.01, Logan, America) was added to a volume of 1 mL. The mixture was homogenized by ultrasonication (KQ3200DB, Shumei, China) for 30 minutes to obtain 10 mg/mL PDA NPs working solution.

Characterization of Polydopamine Nanoparticles

The morphology and size of the prepared PDA NPs were obtained by transmission electron microscope (TEM) (JEM-2100F, Jeol, Japan). The ultraviolet-visible (UV-vis) absorption spectra was recorded on spectrophotometer (UV-2600, Shimadzu, Japan). A thermocouple thermometer (LE-LS-808-10000TFC, Leoptics, China) was used to measure the relationship between the concentration of PDA NPs solution and the power density of near infrared (NIR) laser. The photothermal conversion efficiency was calculated by measuring the temperature change in 2 mL of PDA NPs solution (100 μg/mL) under NIR laser irradiation (3 W/cm^2).[24] A thermal imager (Ti27, Fluke, America) was used to record the temperature change in PDA NPs solution (10 mg/mL) every 30 seconds under NIR laser irradiation (0.48 W/cm^2).

Study Design

Forty-five male Sprague-Dawley (SD) rats (8 weeks of age; 300 g average body weight) were used in the study. They were randomly assigned to the photothermal group, the control group (PBS) and the PDA NPs group (n = 15 per group). The rats were housed individually at room temperature (23–25 °C) with a relative humidity of 45% - 55%, and allowed free access to water and standard food pellets. All experiments including surgery and NIR irradiation were conducted

under general anesthesia via 2.5% isoflurane. The experimental protocol was approved by the Institutional Review Board of the First Hospital of Jilin University (Approval No. 20210064), and all animals care and use followed the Guide for the Care and Use of Laboratory Animals published by the National Institutes of Health (USA).

Surgical Procedure and Photothermal Therapy

After the fur of the hindlimbs was removed, the surgery was performed with the rat in a prone position. Under sterile conditions, a 1.5 cm incision was made longitudinally along the Achilles tendon (Figure 1A). After excising the accessory tendon, the Achilles tendon was transected completely at 5 mm proximal to its insertion into the calcaneus of the foot (Figure 1B). The tendon was sutured immediately using the Kessler technique with 6–0 suture (Round needle 3/8, 2.5 × 8, Yuankang Medical, China) (Figure 1C). A second transection was made in the tendon 3 mm proximal to the suturing site to reduce tensile forces across the repair site to create adhesion formation around the repair site (Figure 1D).

Before the skin was closed, 50 μL of the PDA NPs solution (10 mg/mL) was administrated around the suturing site in the photothermal group and the PDA NPs group, whereas 50 μL of PBS was used in the control group (Figure 1E). The skin was then closed interruptedly using 6–0 resorbable suture (Triangular needle 3/8, 3 × 8, Jinhuan Medical, China) (Figure 1F). The rats were allowed to walk freely in cages after surgery.

On 3, 6, 9 and 12 days postoperatively, the repaired sites in the photothermal group were irradiated for 15 minutes per day by NIR laser (808 nm, 0.48 W/cm^2), respectively. The laser device was placed at 15 cm away from the repaired sites. The temperature of the repair sites was kept at 41 ± 0.5 °C, and was monitored with FLIR T650sc camera (detector resolution: 640×480 pixels, wavelength range: 7.5–14 μm, FLIR Systems, Inc., Wilsonville, Ore.).

Biomechanical Testing

The endpoint of the photothermal therapy was two weeks. In addition to evaluating the mechanical strength of the healed Achilles tendon at two weeks, long-term healing was also evaluated at six weeks (n = 3 per group at each time). The Achilles tendon attached to the distal paw was kept in saline at 4 °C prior to testing. After rewarming at room temperature, the proximal tendon was mounted in the upper clamp and the distal paw was mounted over the lower clamp in the universal tensile testing machine (Instron 5569, USA) with a 2000 N load cell. The repair site of the

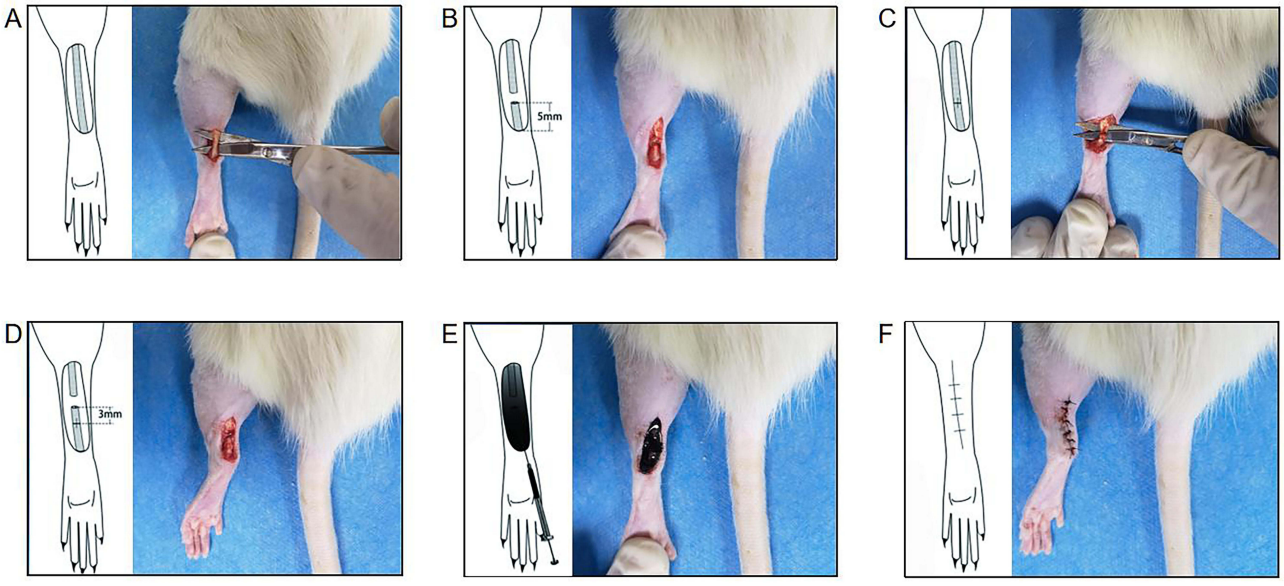

Figure 1 Schematic of the Achilles tendon laceration repair. (**A**) A incision was made longitudinally along the Achilles tendon. (**B**) After excising the accessory tendon, the Achilles tendon was transected completely at 5 mm proximal to its insertion into the calcaneus of the foot. (**C**) The injured tendon was sutured. (**D**) A second transection was made in the tendon 3 mm proximal to the suturing site to reduce tensile forces across the repair site. (**E**) Before the skin was closed, 50 μL of the PDA NPs solution (10 mg/mL) was administrated around the suturing site in the photothermal group and the PDA NPs group, whereas 50 μL of PBS was used in the control group. (**F**) The skin was then closed.

Achilles tendon was kept in the middle of the tested tendon segment, and the specimens were preloaded (0.01 N) and stretched at a constant speed of 10 mm/min until the specimens ruptured.

Histology Examination

At two weeks after surgery, the rats were sacrificed under isoflurane anesthesia followed by cervical dislocation. The skin healed well without infection and ulceration (Supplementary Information Figure 1). The Achilles tendon and its overlying skin were harvested from the musculotendinous junction to the insertion at the calcaneus. Histological staining was used to assess the degree of adhesion formation (n = 5 per group). The sample was fixed in formalin and embedded in paraffin, and then longitudinally cut into two 3 μm slices and stained by hematoxylin and eosin (H&E). According to the grading criteria of Tang et al,[23] adhesion formation of the repair tendon was scored on the basis of the length and density of the fibrotic adhesions by two independent observers, who were blinded to the group allocation. The detailed schematic diagram of the grading criteria of Tang et al had been shown in previous studies.[25]

Immunohistochemistry

Immunohistochemistry (IHC) was conducted to assess the expressions of heat shock protein (Hsp) 72 and α-smooth muscle actin (α-SMA) (n = 5 per group). The same sample was cut into 1.5 μm slices. After de-paraffinization, antigen retrieval and endogenous peroxidase blockage. The sections were incubated with rabbit anti-α-SMA antibody (1: 400; Cell Signaling Technology, Cat# 19245S, Beverly, America) and anti-Hsp 72 antibody (1: 100; Enzo Life Sciences, Cat# ADI-SPA-812-F, New York, America) at 4°C overnight, and then incubated with horseradish peroxidase conjugated goat anti-rabbit IgG (Zhongshan Golden Bridge Biotechnology Co. Ltd, Cat# PV-6001, Beijing, China) for 20 min. Staining results were visualized with diaminobenzidine (Zhongshan Golden Bridge Biotechnology Co. Ltd, Cat# ZLI-9079, Beijing, China) and hematoxylin. The images were taken under light microscope (BX51, Olympus, Japan), five high-power fields (400 ×) were chosen and captured (cellSens Dimension, Olympus, Japan). The images were analysis using Image-Pro Plus 6.0 software.

Western Blot

Western Blot (WB) was conducted to assess the expressions of Hsp 72, c-Jun N-terminal Kinase (JNK), p-JNK and α-SMA (n = 4 per group). The specimens were homogenized on ice and incubated in RIPA lysis buffer (NCM Biotech Co. Ltd, Cat# P0100, Suzhou, China) at 4 °C for 1 h. After centrifugation, the total protein concentration was determined using an Enhanced BCA Protein Assay Kit (Beyotime, Cat# P0010, Shanghai, China). The samples were separated by SDS-PAGE (Dake Wei Biological Engineering Co. Ltd, Cat# 8012011, Shenzhen, China), and then transferred onto polyvinylidene fluoride membranes (GE Healthcare Life Sciences, Cat# 10600023, Freiburg, Germany). After blocked with 5% BSA Albumin Fraction V or 5% skim milk powder, immunoblots were incubated with rabbit polyclonal antibody against p-JNK (1:1000; Cell Signaling Technology, Cat# 4668S, Beverly, America), JNK (1:1000; Cell Signaling Technology, Cat# 9252S, Beverly, America), Hsp 72 (1: 1000; Enzo Life Sciences, Cat# ADI-SPA-812-F, New York, America), α-SMA (1: 500; Cell Signaling Technology, Cat# 19245S, Beverly, America) and GAPDH (1:10,000; Proteintech, Cat# 10494-1-AP, Chicago, America). After washing, IRDye 800CW goat anti-rabbit IgG (1:15,000; LI-COR, Cat#926-32211, Lincoln, America) was added and incubated for 1h. Immunoreactive proteins were detected using an infrared dichroic laser scanning imaging system (Odyssey, LI-COR, America) and densitometry was performed using ImageJ software.

Statistical Analysis

The statistical analysis was evaluated using IBM SPSS Statistics version 25 (IBM Corp., Armonk, America). The data were expressed as mean ± Standard Error of the Mean (SEM). The Shapiro–Wilk test was performed to test for normality, and all dates fit a normal distribution. The failure to load for different groups at two weeks and six weeks after surgery was compared using the one-way analysis of variance (ANOVA) followed by Tukey's test. The difference in adhesion scores, Hsp 72, JNK, p-JNK and α-SMA among groups two weeks after surgery was compared using the one-way ANOVA followed by Tukey's test. A p-value < 0.05 was considered statistically significant.

Results

Characterization of Polydopamine Nanoparticles

The PDA-NPs with photothermal effects were synthesized by a simple one-step alkaline self-polymerization method.[26,27] As shown in Figure 2A, the PDA-NPs showed uniformly dispersed spherical morphology with an average diameter of 143.2 nm. The UV-Vis absorption spectra of PDA-NPs solution revealed a broad peak from 200 nm to over 800 nm (Figure 2B). Under 808nm NIR laser irradiation, the PDA NPs could produce heat rapidly due to its absorption at this wavelength and its ability to convert light energy into heat energy in the form of non-radiative transitions. The temperature increased in PDA-NPs concentration-, irradiation time- and laser power-dependent features (Figure 2C and Figure 2D). The photothermal conversion efficiency was calculated as 61.06% according to heating and cooling

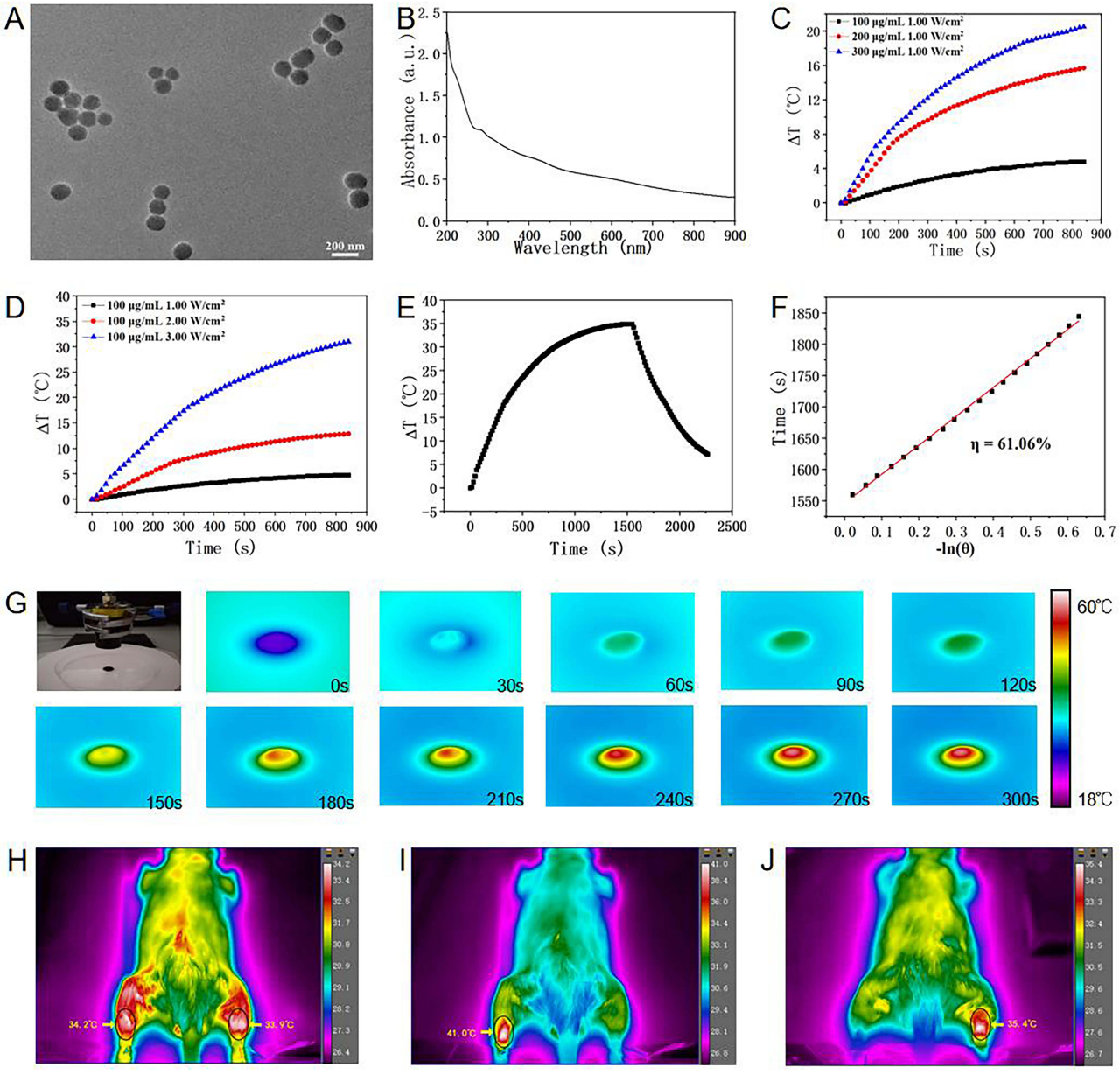

Figure 2 The characterization and photothermal effect of polydopamine nanoparticles (PDA NPs). (**A**) TEM image of PDA nanoparticles. (**B**) UV absorption spectrum of PDA nanoparticle solution. (**C**) The temperature increment of PDA nanoparticle solution with different concentration. (**D**) The temperature increment of PDA nanoparticle solution with different laser power density. (**E**) The heating and cooling curve of PDA nanoparticle solution. (**F**) The calculation of photothermal conversion efficiency. (**G**) The temperature increment of PDA nanoparticle solution (10 mg/mL) under the laser power density of 0.48 W/cm^2. (**H-J**) Thermal images of skin temperature on the surface of the Achilles tendon under different conditions.

curves (Figure 2E and Figure 2F). In particular, the PDA NPs solution at a concentration of 10 mg/mL could reach 53 °C at 300 s at a low NIR laser power density (0.48 W/cm^2) (Figure 2G), which was applied in the subsequent experiments. In vivo studies showed that polydopamine nanoparticles implanted in the left hindlimb does not affect skin temperature when they are not irradiated by NIR laser (Figure 2H). Under NIR laser irradiation, the temperature in the repair site rapidly reaches 41 °C (Figure 2I). NIR laser irradiation does not reach 41 °C in the contralateral hindlimb without polydopamine nanoparticles (Figure 2J).

Polydopamine Nanoparticles-Based Photothermal Effect Did Not Affect Tendon Healing

Figure 3 illustrates the mechanical strength during tendon rupture (n = 3 per group at each time point). We tested the load of tendon rupture was not significant across three groups at two weeks after surgery (Figure 3A) (Photothermal: 57.81 ± 3.15 N; Control: 44.06 ± 8.16 N; PDA NPs: 49.31 ± 2.69 N) (F = 1.72, p = 0.256) and the load of tendon rupture was not significant across three groups at six weeks after surgery (Figure 3B) (Photothermal: 85.37 ± 3.70 N; Control: 81.76 ± 4.96 N; PDA NPs: 81.89 ± 4.14 N) (F = 0.23, p = 0.804), too.

Polydopamine Nanoparticles-Based Photothermal Effect Decreased Adhesion Scores

Figure 4 illustrates adhesion scores for each group at two weeks after surgery (n = 5 per group). We observed a statistically significant difference in adhesion scores among the groups (F = 10.74, p = 0.002). Results from Tukey's comparisons indicated that the adhesion score was significantly decreased in the photothermal group (4.25 ± 0.21), followed by the control group (5.29 ± 0.12) and the PDA NPs group (5.29 ± 0.20) (Photothermal vs Control: p = 0.005; Photothermal vs PDA NPs: p = 0.005; Control vs PDA NPs: p > 0.05).

Polydopamine Nanoparticles-Based Photothermal Effect Enhanced the Expression of Hsp 72

Figure 5 illustrates the Hsp 72 expression in the repaired tendons was measured by immunohistochemistry (n = 5 per group) and Western blot (n = 4 per group) at two weeks after surgery. Figure 5A and Figure 5B illustrate a significant difference was observed in Hsp 72 across the three groups (F = 9.36, p = 0.004). The post hoc Tukey's test found that the highest expression of Hsp 72 was within the photothermal group (0.104 ± 0.10), followed by the control group (0.062 ± 0.01) and then the PDA NPs group (0.052 ± 0.01) (Photothermal vs Control: p = 0.016; Photothermal vs PDA NPs: p = 0.004; Control vs PDA NPs: p > 0.05). Figure 5C and Figure 5D illustrate a significant difference was also observed in Hsp 72 across the three groups (F = 12.93, p = 0.002). The post hoc Tukey's test found that the highest expression of Hsp 72 was within the photothermal group (0.790 ± 0.06), followed by the control group (0.545 ± 0.04) and the PDA NPs

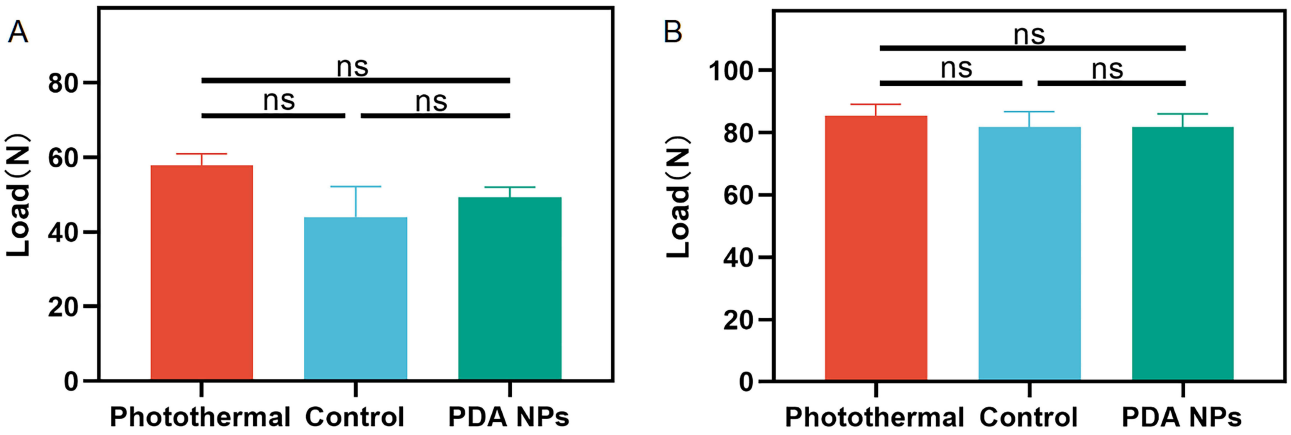

Figure 3 Polydopamine nanoparticles-based photothermal effect did not affect tendon healing. (**A**) The load of tendon rupture at two weeks after surgery. (**B**) The load of tendon rupture at six weeks after surgery. The bars represent mean ± SEM (n = 3 per group). ns, not significant.

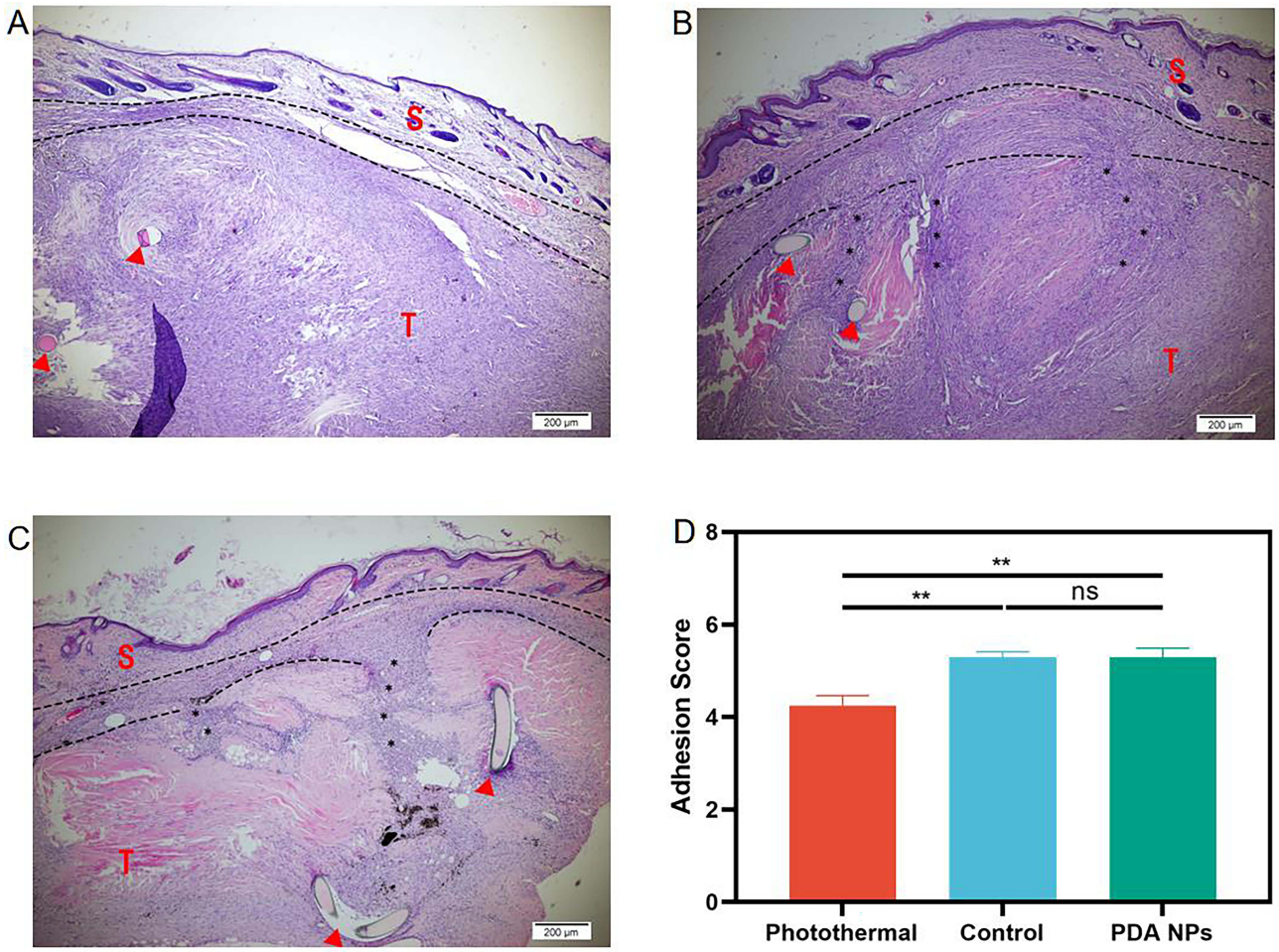

Figure 4 Histological assessment on adhesion formation (40 ×). (**A**) In the photothermal group, there is an interval between the skin (S) and the repaired tendon (T) at the repair site (Arrowhead), but the interval disappeared and was filled by dense scar in the control group (**B**) and the PDA NPs group (**C**). (**D**) Average adhesion score in the photothermal group is significantly lower than that in the control group and the PDA NPs group. The data is expressed by mean ± SEM (one-way ANOVA, $p = 0.002$; $n = 5$ per group). ** $p < 0.01$; ns, no significant.

group (0.528 ± 0.02) (Photothermal vs Control: $p = 0.005$; Photothermal vs PDA NPs: $p = 0.004$; Control vs PDA NPs: $p > 0.05$).

Polydopamine Nanoparticles-Based Photothermal Effect Blocked Phosphorylation of JNK

Figure 6 illustrates the JNK and p–JNK expression in the repaired tendons was measured by Western blot ($n = 4$ per group) at two weeks after surgery. Although the expression of JNK were not found to be different across three groups (Photothermal: 3.460 ± 0.32; Control: 4.188 ± 0.30; PDA NPs: 4.080 ± 0.39) ($F = 1.37$, $p = 0.303$), p-JNK was significantly lower in the photothermal group (0.233 ± 0.05) than that in the control group (0.488 ± 0.04) and the PDA NPs group (0.630 ± 0.06) ($F=16.16$, $p = 0.001$) (Photothermal vs Control: $p = 0.014$; Photothermal vs PDA NPs: $p = 0.001$; Control vs PDA NPs: $p > 0.05$).

Polydopamine Nanoparticles-Based Photothermal Effect Inhibited Fibroblast-to-Myofibroblast Transition

Figure 7 illustrates the α-SMA expression in the repaired tendons was measured by immunohistochemistry ($n = 5$ per group) and Western blot ($n = 4$ per group) at two weeks after surgery. Figure 7A and Figure 7B illustrate a significant

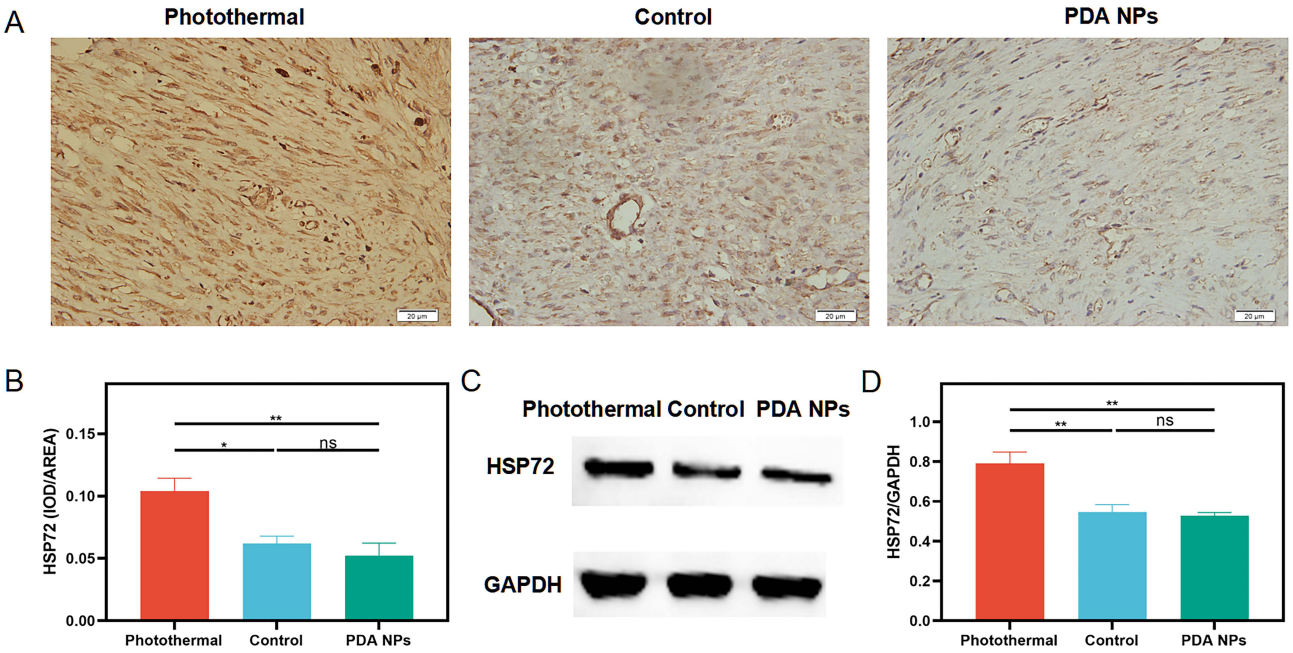

Figure 5 The Hsp 72 expression in the repaired tendons was measured by immunohistochemistry (n = 5 per group) and Western blot (n = 4 per group) at two weeks after surgery. (**A**) Immunohistochemical evaluation of Heat shock protein (Hsp) 72 (400 ×). (**B**) Average Hsp 72 in the photothermal group increases significantly compared with the other two groups (mean ± SEM; one-way ANOVA, p = 0.004; n = 5 per group). (**C**) Western blot of Heat shock protein (Hsp) 72. (**D**) Average Hsp 72 in the photothermal group increases significantly relative to the other two groups (mean ± SEM; one-way ANOVA, p = 0.002; n = 4 per group). * p < 0.05; ** p < 0.01; ns, no significant.

difference was observed in α-SMA across the three groups (F = 13.58, p = 0.001). The post hoc Tukey's test found that the lowest expression of α-SMA was within the photothermal group (0.070 ± 0.01), followed by the control group (0.112 ± 0.01) and then the PDA NPs group (0.110 ± 0.003) (Photothermal vs Control: p = 0.002; Photothermal vs PDA NPs:

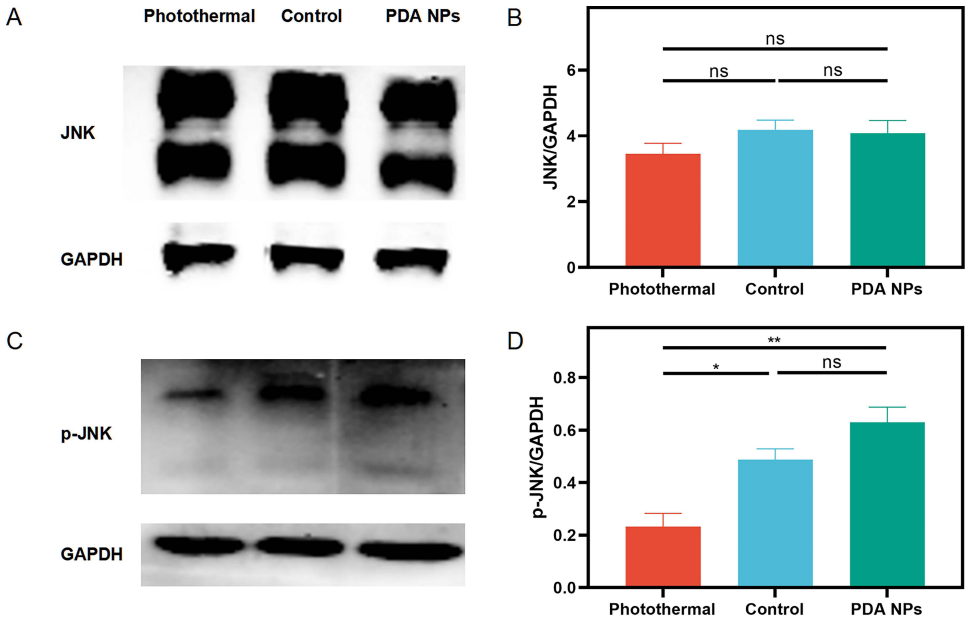

Figure 6 The JNK and p–JNK expression in the repaired tendons was measured by Western blot (n = 4 per group) at two weeks after surgery. (**A** and **C**) Western blot of Jun N-terminal kinase (JNK) and phospho-JNK (p-JNK). (**B**) There is no significant difference in JNK across three groups (mean ± SEM; one-way ANOVA, p = 0.303; n = 4 per group), (**D**) but p-JNK in the photothermal group decreases significantly (mean ± SEM; one-way ANOVA, p = 0.001; n = 4 per group). * p < 0.05; ** p < 0.01; ns, no significant.

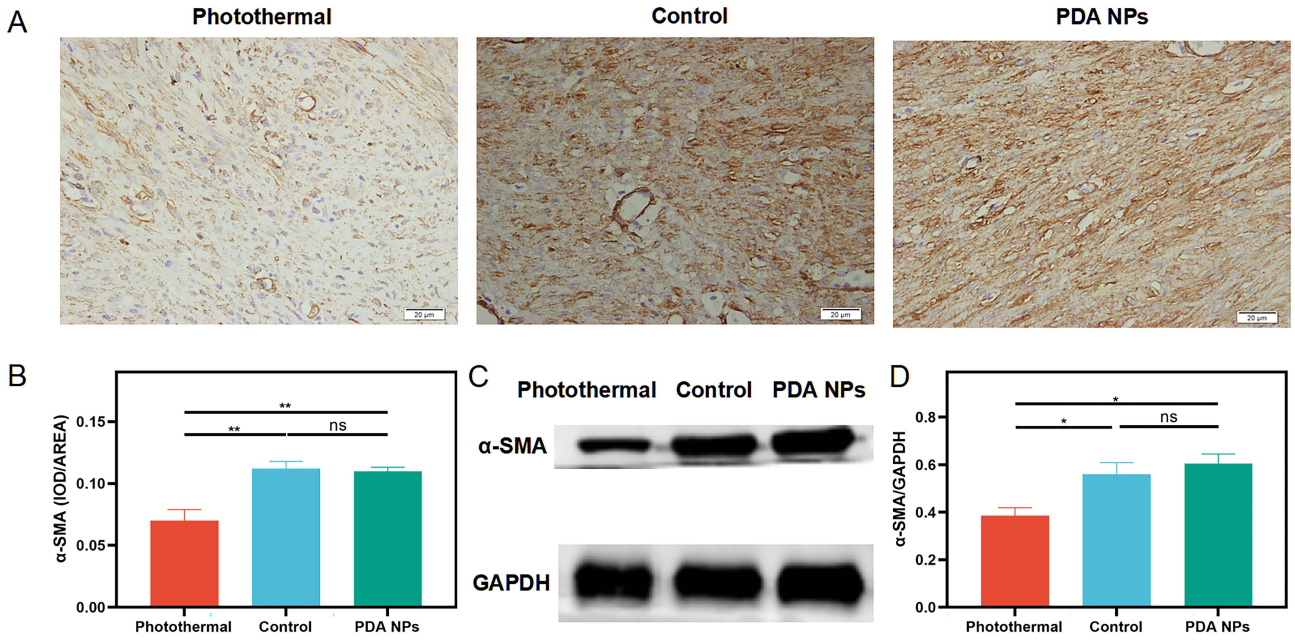

Figure 7 The α-SMA expression in the repaired tendons was measured by immunohistochemistry (n = 5 per group) and Western blot (n = 4 per group) at two weeks after surgery. (**A**) Immunohistochemical evaluation of α- smooth muscle actin (α-SMA) (400 ×). (**B**) Average α-SMA in the photothermal group decreases significantly compared with the other two groups (mean ± SEM; one-way ANOVA, p = 0.001; n = 5 per group). (**C**) Western blot of α-SMA. (**D**) Average α-SMA in the photothermal group decreases significantly relative to the other two groups (mean ± SEM; one-way ANOVA, p = 0.011; n = 4 per group). * p < 0.05; ** p < 0.01; ns, no significant.

p = 0.002; Control vs PDA NPs: p > 0.05). Figure 7C and Figure 7D illustrate a significant difference was also observed in α-SMA across the three groups (F = 7.84, p = 0.011). The post hoc Tukey's test found that the lowest expression of α-SMA was within the photothermal group (0.385 ± 0.03), followed by the control group (0.560 ± 0.05) and then the PDA NPs group (0.605 ± 0.04) (Photothermal vs Control: p = 0.037; Photothermal vs PDA NPs: p = 0.011; Control vs PDA NPs: p > 0.05).

Discussion

Photothermal therapy is a kind of light-activated, photothermal reagent based modality, which involves administration of exogenous photothermal reagent as light absorbers and in vitro irradiation with NIR laser (650–900 nm).[26–28] It has been used in biomedical fields such as antitumor and antimicrobial.[27] However, its role in the prevention of adhesion formation after tendon injury has not been investigated. The structure of PDA NPs is similar to natural melanin, advantages of PDA NPs include its prominent biocompatibility, excellent biodegradability, good photostability, strong light absorption capacity, prominent near-infrared thermal conversion, long-term safety and ease of synthesis.[29–32] Based on the above advantages, we used PDA NPs as the photothermal material in this study.

Injured tendon initiates inflammatory response and inflammatory cells infiltrate into the subcutaneous tissue and the tendon. These inflammatory cells activate the resident fibroblasts. The present study found that the PDA NPs photothermal effects attenuate adhesion formation after tendon injury by increasing Hsp 72 expression and reducing myofibroblasts in a rat model of the Achilles tendon laceration repair. The degree of adhesion was significantly lower in the photothermal group than in the control group and the PDA NPs group, with a net reduction of 1.040 in the adhesion scores. The possible mechanism is that Hsp 72 blocks phosphorylation of JNK, which in turn inhibits the proliferation of fibroblasts (Figure 8).

In this study, we found that the protein level of Hsp 72 was obviously upregulated, but phospho-JNK was significantly downregulated in the photothermal therapy group when compared with the other two groups. This suggested that Hsp 72 might contribute to the protection of photothermal therapy against tendon scar formation, which might be mediated by inhibiting phosphorylation of JNK. Accumulating evidences have demonstrated that open injury leads to

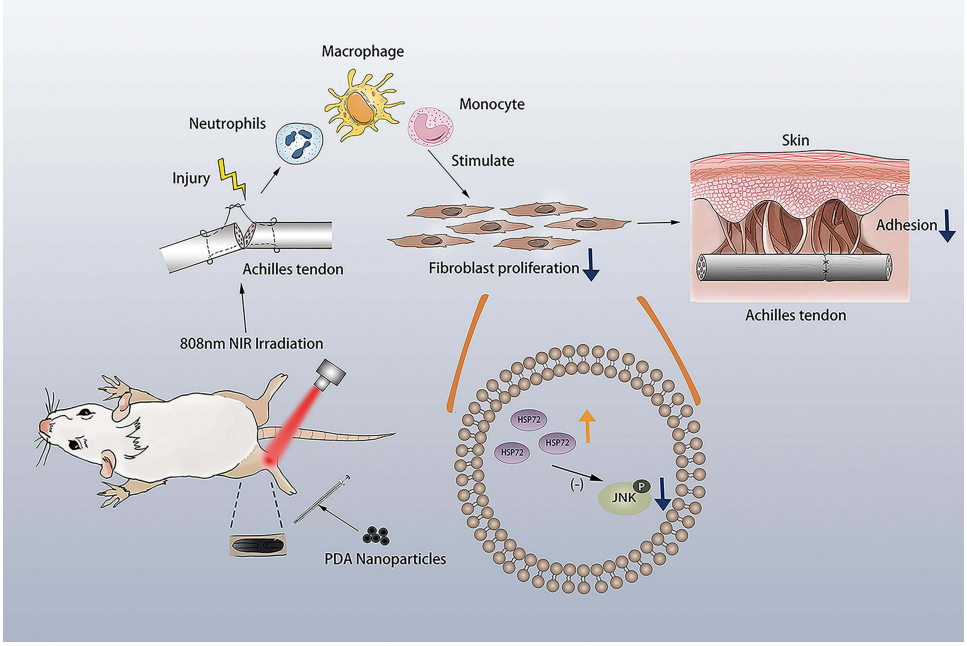

Figure 8 A possible mechanism of action of photothermal effect against adhesion formation after tendon injury.

oxidative stress, which is characterized with intracellular accumulation of reactive oxygen species (ROS). Apart from profibrotic cytokines such as TGF-β1, ROS is a primary factor leading to JNK activation. It was reported that Hsp72 inhibited liver injury via attenuation of oxidative stress-dependent JNK activation.[33] As an inducible protein chaperone, Hsp72 could mitigate endoplasmic reticulum (ER) stress by prevention of misfolded protein aggregation.[34] Notably, intracellular ROS was also abnormally increased under the condition of ER stress. It was reported that mitigation of ER stress with chemical chaperone 4-PBA significantly alleviated oxygen glucose deprivation-triggered generation of ROS in human SH-SY5Y cells.[35] Although we did not investigate the role of Hsp72 in regulation of oxidative stress in this study, these previous studies suggest that the inhibitory effect of Hsp72 on JNK activation might be associated with inhibition of ER stress-dependent generation of ROS.

Reich et al have demonstrated that inhibition of JNK activation could block the conversion from fibroblasts to myofibroblast simulated by TGF-β1.[17] In this study, we found that the expression of α-SMA was significantly down-regulated in the photothermal group when compared with the other two groups. Because the rat model in the study was an extrasynovial flexor injury, adhesion existed between injured tendon and subcutaneous tissue. Its formation is associated with myofibroblasts. In open injury, myofibroblasts arise from resident fibroblasts, which migrate into the provisional matrix consisted of fibrin and fibronectin and are activated by TGF-β1 to acquire a myofibroblastic phenotype.[18] Subsequently, myofibroblasts synthesize and deposit extracellular matrix to replace the provisional matrix and result in adhesion formation.[18] In the process of wound healing, although TGF-β1 has a profibrotic effect, it also plays a crucial role in inducing synthesis of collagens type I and III.[18,36] Thus, complete blockage of TGF-β1 could lead to poor healing of the repaired tendon because collagens type I is a dominant collagen to restore tensile strength and integrity of injured tissue. Wu et al demonstrated that although inhibition of TGF-β1 could attenuate adhesion formation after tendon injury, it simultaneously weakened the tensile strength of the repaired tendon.[14] In the study, macroscopic observation showed that the tendon healed completely (Supplementary Information Figure 2), and we tested the tensile strength of repaired tendons at two weeks and six weeks. Biomechanical testing results showed that polydopamine nanoparticles-based photothermal effect against adhesion formation without affecting tendon healing.

Conclusion

The photothermal effect generated by PDA NPs could attenuate adhesion in a rat model of Achilles tendon laceration. Its possible mechanism is that Hsp72 blocks phosphorylation of JNK, which in turn inhibits the proliferation of fibroblasts. Our results may provide a new direction for future work to develop endogenous heating for postsurgical tissue adhesions, but the photothermal effect against adhesion formation after tendon injury needs further investigation in larger animals.

Acknowledgments

We would like to appreciate the technical help from the Central Laboratory and Department of Pathology, the First Hospital (Section 2) of Jilin University.

The preparation and characterization of PDA NPs were performed by State Key Laboratory of Supramolecular Structure and Materials, College of Chemistry, Jilin University.

We would like to thank Professor Pengfei Ge, Department of Neurosurgery, First Hospital of Jilin University, and Professor Hao Zhang, State Key Laboratory of Supramolecular Structure and Materials, College of Chemistry, Jilin University, for their important insights in the discussion section.

Disclosure

The authors report no conflicts of interest in this work.

References

1. Voleti PB, Buckley MR, Soslowsky LJ. Tendon healing: repair and regeneration. *Annu Rev Biomed Eng*. 2012;14(1):47–71. doi:10.1146/annurev-bioeng-071811-150122
2. Titan AL, Foster DS, Chang J, Longaker MT. Flexor Tendon: development, Healing, Adhesion Formation, and Contributing Growth Factors. *Plast Reconstr Surg*. 2019;144(4):639e–647e. doi:10.1097/prs.0000000000006048
3. Vucekovich K, Gallardo G, Fiala K. Rehabilitation after flexor tendon repair, reconstruction, and tenolysis. *Hand Clin*. 2005;21(2):257–265. doi:10.1016/j.hcl.2004.11.006
4. Moran SL, Ryan CK, Orlando GS, Pratt CE, Michalko KB. Effects of 5-fluorouracil on flexor tendon repair. *J Hand Surg Am*. 2000;25(2):242–251. doi:10.1053/jhsu.2000.jhsu25a0242
5. Tang JB, Cao Y, Zhu B, Xin KQ, Wang XT, Liu PY. Adeno-associated virus-2-mediated bFGF gene transfer to digital flexor tendons significantly increases healing strength. an in vivo study. *J Bone Joint Surg Am*. 2008;90(5):1078–1089. doi:10.2106/jbjs.F.01188
6. Chen CH, Zhou YL, Wu YF, Cao Y, Gao JS, Tang JB. Effectiveness of microRNA in Down-regulation of TGF-beta gene expression in digital flexor tendons of chickens: in vitro and in vivo study. *J Hand Surg Am*. 2009;34(10):1777–84.e1. doi:10.1016/j.jhsa.2009.07.015
7. Zhao C, Zobitz ME, Sun YL, et al. Surface treatment with 5-fluorouracil after flexor tendon repair in a canine in vivo model. *J Bone Joint Surg Am*. 2009;91(11):2673–2682. doi:10.2106/jbjs.H.01695
8. de Wit T, de Putter D, Tra WM, et al. Auto-crosslinked hyaluronic acid gel accelerates healing of rabbit flexor tendons in vivo. *J Orthop Res*. 2009;27(3):408–415. doi:10.1002/jor.20730
9. Zhao C, Sun YL, Kirk RL, et al. Effects of a lubricin-containing compound on the results of flexor tendon repair in a canine model in vivo. *J Bone Joint Surg Am*. 2010;92(6):1453–1461. doi:10.2106/jbjs.I.00765
10. Tan V, Nourbakhsh A, Capo J, Cottrell JA, Meyenhofer M, O'Connor JP. Effects of nonsteroidal anti-inflammatory drugs on flexor tendon adhesion. *J Hand Surg Am*. 2010;35(6):941–947. doi:10.1016/j.jhsa.2010.02.033
11. Hung LK, Fu SC, Lee YW, Mok TY, Chan KM. Local vitamin-C injection reduced tendon adhesion in a chicken model of flexor digitorum profundus tendon injury. *J Bone Joint Surg Am*. 2013;95(7):e41. doi:10.2106/jbjs.K.00988
12. Zhao C, Ozasa Y, Shimura H, et al. Effects of lubricant and autologous bone marrow stromal cell augmentation on immobilized flexor tendon repairs. *J Orthop Res*. 2016;34(1):154–160. doi:10.1002/jor.22980
13. Orner CA, Geary MB, Hammert WC, O'Keefe RJ, Loiselle AE. Low-Dose and Short-Duration Matrix Metalloproteinase 9 Inhibition Does Not Affect Adhesion Formation during Murine Flexor Tendon Healing. *Plast Reconstr Surg*. 2016;137(3):545e–553e. doi:10.1097/01.prs.0000475823.01907.53
14. Wu YF, Mao WF, Zhou YL, Wang XT, Liu PY, Tang JB. Adeno-associated virus-2-mediated TGF-β1 microRNA transfection inhibits adhesion formation after digital flexor tendon injury. *Gene Ther*. 2016;23(2):167–175. doi:10.1038/gt.2015.97
15. Fatemi MJ, Shirani S, Sobhani R, et al. Prevention of Peritendinous Adhesion Formation After the Flexor Tendon Surgery in Rabbits: a Comparative Study Between Use of Local Interferon-α, Interferon-β, and 5-Fluorouracil. *Ann Plast Surg*. 2018;80(2):171–175. doi:10.1097/sap.0000000000001169
16. Wong JK, Lui YH, Kapacee Z, Kadler KE, Ferguson MW, McGrouther DA. The cellular biology of flexor tendon adhesion formation: an old problem in a new paradigm. *Am J Pathol*. 2009;175(5):1938–1951. doi:10.2353/ajpath.2009.090380
17. Reich N, Tomcik M, Zerr P, et al. Jun N-terminal kinase as a potential molecular target for prevention and treatment of dermal fibrosis. *Ann Rheum Dis*. 2012;71(5):737–745. doi:10.1136/annrheumdis-2011-200412
18. Lebonvallet N, Laverdet B, Misery L, Desmoulière A, Girard D. New insights into the roles of myofibroblasts and innervation during skin healing and innovative therapies to improve scar innervation. *Exp Dermatol*. 2018;27(9):950–958. doi:10.1111/exd.13681

19. Hinz B, Phan SH, Thannickal VJ, et al. Recent developments in myofibroblast biology: paradigms for connective tissue remodeling. *Am J Pathol*. 2012;180(4):1340–1355. doi:10.1016/j.ajpath.2012.02.004
20. Wang Y, He G, Tang H, et al. Aspirin inhibits inflammation and scar formation in the injury tendon healing through regulating JNK/STAT-3 signalling pathway. *Cell Prolif*. 2019;52(4):e12650. doi:10.1111/cpr.12650
21. Gabai VL, Meriin AB, Mosser DD, et al. Hsp70 prevents activation of stress kinases. A novel pathway of cellular thermotolerance. *J Biol Chem*. 1997;272(29):18033–18037. doi:10.1074/jbc.272.29.18033
22. Healy C, Mulhall KJ, Fitz Patrick D, Kay EW, Bouchier-Hayes D. The effect of thermal preconditioning of the limb on flexor tendon healing. *J Hand Surg Eur Vol*. 2007;32(3):289–295. doi:10.1016/j.Jhsb.2007.01.004
23. Tang JB, Ishii S, Usui M, Aoki M. Dorsal and circumferential sheath reconstructions for flexor sheath defect with concomitant bony injury. *J Hand Surg Am*. 1994;19(1):61–69. doi:10.1016/0363-5023(94)
24. Xu N, Hu A, Pu X, et al. Fe(III)-Chelated Polydopamine Nanoparticles for Synergistic Tumor Therapies of Enhanced Photothermal Ablation and Antitumor Immune Activation. *ACS Appl Mater Interfaces*. 2022;14(14):15894–15910. doi:10.1021/acsami.1c24066
25. Li S, Gong F, Zhou Z, Gong X. Combined Verapamil-Polydopamine Nanoformulation Inhibits Adhesion Formation in Achilles Tendon Injury Using Rat Model. *Int J Nanomedicine*. 2023;18:115–126. doi:10.2147/ijn.S377600
26. Ge R, Lin M, Li X, et al. Cu(2+)-Loaded Polydopamine Nanoparticles for Magnetic Resonance Imaging-Guided pH- and Near-Infrared-Light-Stimulated Thermochemotherapy. *ACS Appl Mater Interfaces*. 2017;9(23):19706–19716. doi:10.1021/acsami.7b05583
27. Li X, Lovell JF, Yoon J, Chen X. Clinical development and potential of photothermal and photodynamic therapies for cancer. *Nat Rev Clin Oncol*. 2020;17(11):657–674. doi:10.1038/s41571-020-0410-2
28. Happonen E, Tamarov K, Martikainen MV, et al. Thermal dose as a universal tool to evaluate nanoparticle-induced photothermal therapy. *Int J Pharm*. 2020;587:119657. doi:10.1016/j.ijpharm.2020.119657
29. Qi X, Xiang Y, Cai E, et al. All-in-one: harnessing multifunctional injectable natural hydrogels for ordered therapy of bacteria-infected diabetic wounds. *Chem Eng J*. 2022;439:135691. doi:10.1016/j.cej.2022.135691
30. Li Z, You S, Mao R, et al. Architecting polyelectrolyte hydrogels with Cu-assisted polydopamine nanoparticles for photothermal antibacterial therapy. *Mater Today Bio*. 2022;15:100264. doi:10.1016/j.mtbio.2022.100264
31. Qi X, Huang Y, You S, et al. Engineering Robust Ag-Decorated Polydopamine Nano-Photothermal Platforms to Combat Bacterial Infection and Prompt Wound Healing. *Adv Sci*. 2022;9(11):e2106015. doi:10.1002/advs.202106015
32. Zeng Q, Qian Y, Huang Y, Ding F, Qi X, Shen J. Polydopamine nanoparticle-dotted food gum hydrogel with excellent antibacterial activity and rapid shape adaptability for accelerated bacteria-infected wound healing. *Bioact Mater*. 2021;6(9):2647–2657. doi:10.1016/j.bioactmat.2021.01.035
33. Levada K, Guldiken N, Zhang X, et al. Hsp72 protects against liver injury via attenuation of hepatocellular death, oxidative stress, and JNK signaling. *J Hepatol*. 2018;68(5):996–1005. doi:10.1016/j.jhep.2018.01.003
34. Rosas PC, Nagaraja GM, Kaur P, et al. Hsp72 (HSPA1A) Prevents Human Islet Amyloid Polypeptide Aggregation and Toxicity: a New Approach for Type 2 Diabetes Treatment. *PLoS One*. 2016;11(3):e0149409. doi:10.1371/journal.pone.0149409
35. Wang HF, Wang ZQ, Ding Y, et al. Endoplasmic reticulum stress regulates oxygen-glucose deprivation-induced parthanatos in human SH-SY5Y cells via improvement of intracellular ROS. *CNS Neurosci Ther*. 2018;24(1):29–38. doi:10.1111/cns.12771
36. Biernacka A, Dobaczewski M, Frangogiannis NG. TGF-β signaling in fibrosis. *Growth Factors*. 2011;29(5):196–202. doi:10.3109/08977194.2011.595714